Supplementary Materials

Molecular Biology of the Cell

Vitale *et al*.

Supplementary Figures

Supplementary Figure 1. Domain organization of Brl1 like proteins from the indicated organisms. Predictions from the AlphaFold Protein Structure Database show that AαH and DAH are conserved in these Brl1/Brr6 like proteins (left). Heliquest predictions for the AαH in the perinuclear space are shown on the right (Gautier *et al.*, 2008). (A) *Saccharomyces cerevisiae - BRR6*. (B) *Saccharomyces pombe - brr6.* (C) *Candida albicans - brr6 like C-C domain containing protein*. (D) *Plasmodium falciparum - BRR6.*

Supplementary Figure 2. Role of AαH and DAH for the function of Brl1 and the BRL1 overexpression phenotype. (A) Domain organization of Brl1 with the analyzed mutations in the DAH (enlargement on top). Conserved (blue) and not conserved (red) amino acids and the introduced amino acid changes (Supplementary Figure S2B-D) are indicated (Gardner *et al.*, 2021). (B) Growth test of *BRL1* and indicated *BRL1* mutants using a plasmid shuffle approach. 10-fold serial dilutions were spotted onto SC-Leu and 5-FOA plates that were incubated at the indicated temperatures. (C) Cells with the indicated P_{Gal1} plasmids were grown on glucose (Glu) and galactose/raffinose (Gal/Raf) plates at 30°C for 2 days. P_{Gal1}-*brl1*^{F391P} and the combination of P_{Gal1}-*brl1*$^{F391E\ DAH}$ cells showed the same toxicity of P_{Gal1}-*brl1*^{F391E} upon promoter induction. Slight toxic effect was observed for P_{Gal1}-*brl1*^{C347Y} *and* P_{Gal1}-*brl1*$^{C365S\ C371S}$ overexpression. (D) Microscopic analysis of cells carrying dsRED-HDEL and the indicated P_{Gal1} plasmids. Cells were grown in raffinose overnight followed by the addition of galactose for 3 h at 30°C to induce P_{Gal1}. Scale bar: 3 µm. (E, F) P_{Gal1}-*brl1*^{F391E} was induced for 3-5 h by the addition of galactose to cells grown in raffinose medium at 30ºC. (E) Morphology of petals attached with the NE. (F) Petals that detached from the NE. Scale bars: 400 nm.

Supplementary Figure 3. Overexpression toxicity of P_{Gal1}-*brl1*^{F391E} is not dependent on *APQ12, BRR6* or *NUP116*. (A-C) WT, *apq12*Δ*, apq12-ah* cells (A), *brr6-751* cells (C) and *nup116*Δ cells with the indicated P_{Gal1} plasmids were grown on glucose (Glu) and galactose/raffinose (Gal/Raf) plates at 30ºC for 2 days.

Supplementary Figure 4. NPC phenotype of P_{Gal1}-*brl1*^{F391E} cells with and without induction of the P_{Gal1} promoter. (A) *NUP159-tdTomato*, *NSP1-tdTomato*, *NUP82-tdTomato* and *NUP42-tdTomato* cells with *yeGFP*, *BRL1-yeGFP* or *brl1*^{F391E}*-yeGFP* under control of the P_{Gal1} promoter grown in raffinose medium at 30ºC. Scale bar: 5 µm. (B) Line scan of the NE of enlarged cells shown in Figure 4B (*NUP159-tdTomato*, *NSP1-tdTomato*, *NUP82-tdTomato*) and Figure 4C (*NUP42-tdTomato*). (C) Distribution of Nup159-yeGFP and Nup82-tdTomato carrying P_{Gal1}, P_{Gal1}-*BRL1* or P_{Gal1}-*brl1*^{F391E} under control of the P_{Gal1} promoter grown in raffinose medium at 30ºC. Line scans on the bottom show distribution of the yeGFP and tdTomato signals. The yellow asterisk (*) corresponds to the enlarged cell on the right used for the scan analysis of the NE. *NUP159-yeGFP NUP82-tdTomato* cells under P_{Gal1} promoter induction condition (3 h) are shown in Figure 4E. Scale bar: 5 µm.

Supplementary Figure 5. Impact of P_{Gal1}-*brl1*^{F391E}*-yeGFP* overexpression on Nup133, Nup84, and Nup116. (A) *NUP133-tdTomato*, *NUP84-tdTomato* and *NUP116-tdTomato* cells with *yeGFP*, *BRL1-yeGFP* or *brl1*^{F391E}*-yeGFP* under control of the P_{Gal1} promoter grown in raffinose/galactose medium at 30ºC for 0 h and 3 h.

Line scans of tdTomato signal along the NE are shown on the right. (B) *NUP159-yeGFP NUP116-tdTomato* cells with P_{Gal1}, P_{Gal1}-*BRL1* or P_{Gal1}-*brl1*^{F391E} grown in raffinose/galactose medium at 30ºC for 0 h and 3 h. The yellow asterisk (*) indicates the cell used for the line scan analysis of yeGFP and tdTomato signal along the NE. The interested cell is showed enlarged on the right. (A, B) Scale bars: 5 µm.

Supplementary Figure 6. SIM analysis. Impact of P_{Gal1}-*BRL1* P_{Gal1}-*brl1*^{F391E} overexpression on Nup159, Nup82, Nsp1, Nup42 tagged with tdTomato fixed with 4% PFA and 2% Sucrose and analysed with SIM super resolution microscopy**.** Scale bars: 2 µm.

Supplementary Figure 7. Core NPC assembly is not affected by P_{Gal1}-*brl1*^{F391E} overexpression. (A) Experimental outline of RITE assay. (B) Estradiol induces a Cre-induced recombination switch of *NUP188-mCherry* (old) to *NUP188-yeGFP* (new). P_{Gal1}, P_{Gal1}-*BRL1* and P_{Gal1}-*brl1*^{F391E} cells carrying the NUP188mCherry-yeGFP RITE construct were grown for 2 h in the presence of galactose and estradiol at 30ºC. Cells were analysed by fluorescence microscopy. Scale bar: 5 µm.

Supplementary Figure 8. Immuno-EM control and MAB414 analysis of P_{Gal1}-*brl1*^{F391E} cells by immuno-EM. (A) WT cells not expressing yeGFP were incubated with anti-GFP antibodies followed by Protein A-gold (15 nm). No gold staining was observed in 10 inspected yeast cells. Two representative cells are shown. Scale bar: 200 nm. (B) MAB414 staining of P_{Gal1}-*brl1*^{F391E} cells. Cells overexpressing P_{Gal1}-*brl1*^{F391E} for 3 h were fixed and then incubated with MAB414 followed by Protein A-gold (15 nm). Cells were analysed by EM. Scale bar: (top panel) 200 nm, (bottom panel) 500 nm, enlargements; 200 nm.

A

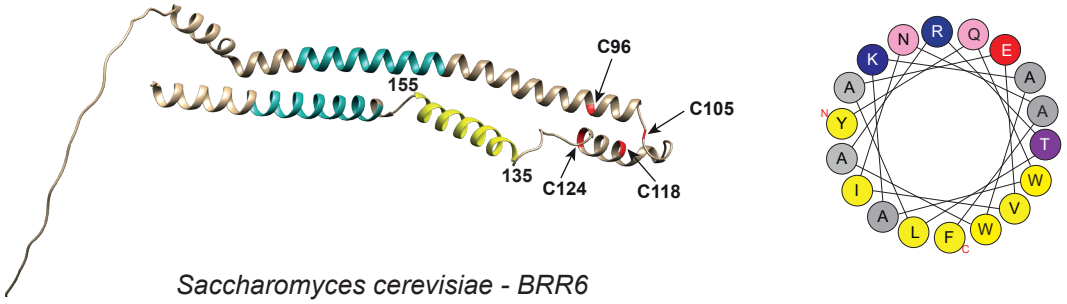

Saccharomyces cerevisiae - BRR6

B

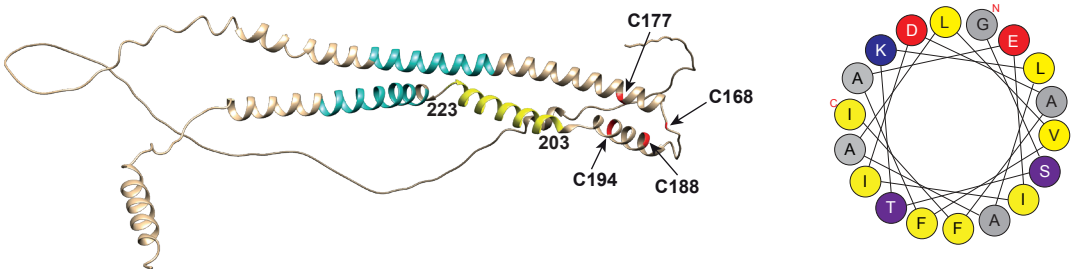

Schizosaccharomyces pombe - brr6

C

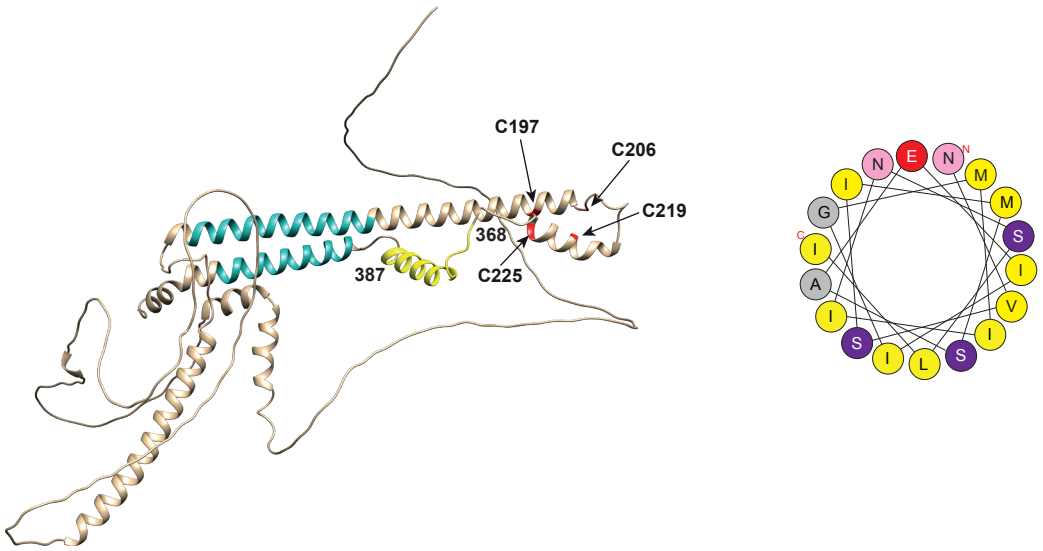

Candida albicans - brr6 like C-C domain containing protein

D

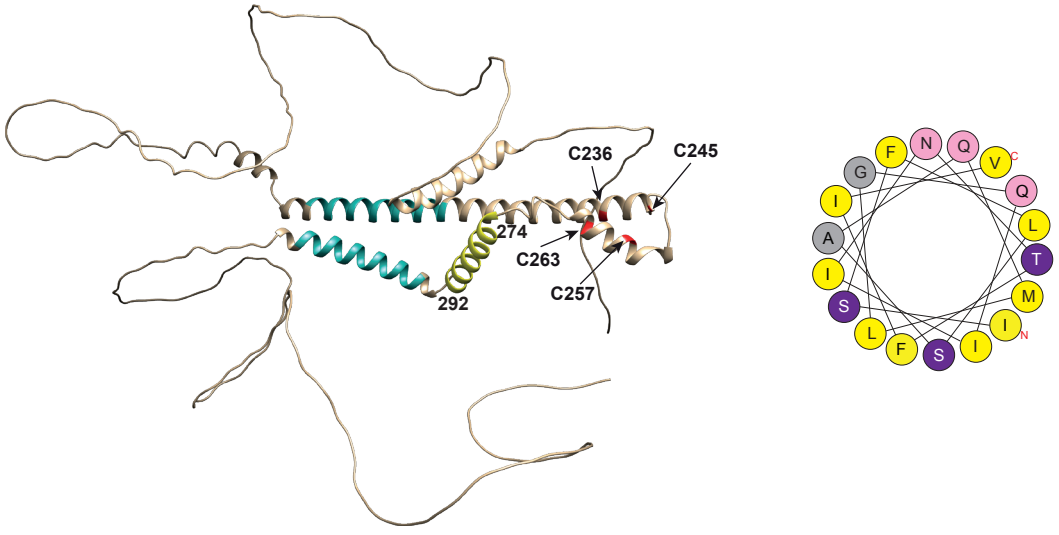

Plasmodium falciparum - BRR6

Figure S2

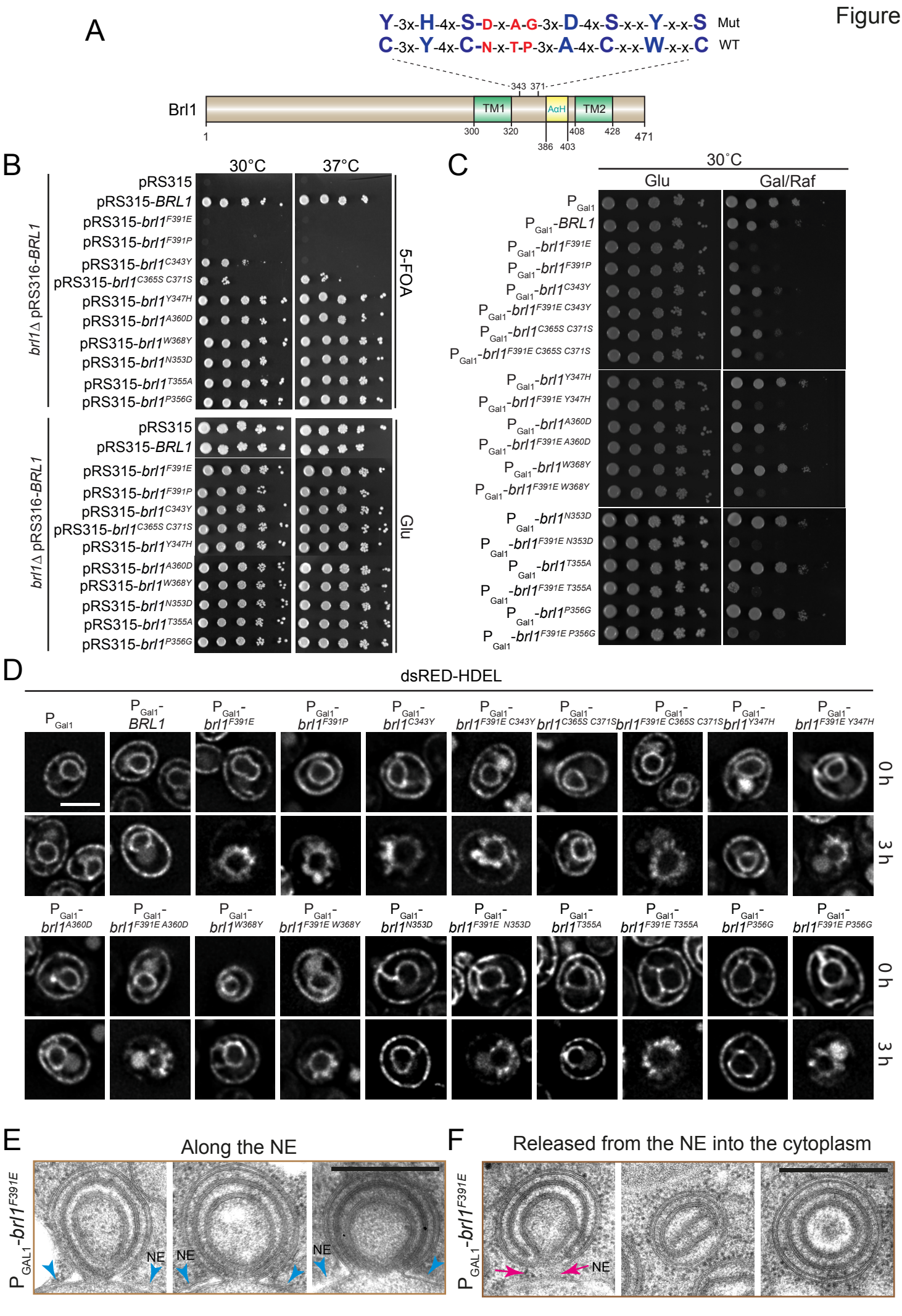
A
Y-3x-H-4x-S-D-x-A-G-3x-D-4x-S-x-x-Y-x-x-S Mut
C-3x-Y-4x-C-N-x-T-P-3x-A-4x-C-x-x-W-x-x-C WT
343 371
Brl1
TM1
AαH
TM2
1
300
320
386
403
408
428
471
B
30°C
37°C
brl1Δ pRS316-BRL1
pRS315
pRS315-BRL1
pRS315-brl1F391E
pRS315-brl1F391P
pRS315-brl1C343Y
pRS315-brl1C365S C371S
pRS315-brl1Y347H
pRS315-brl1A360D
pRS315-brl1W368Y
pRS315-brl1N353D
pRS315-brl1T355A
pRS315-brl1P356G
5-FOA
Glu
C
30˚C
Glu
Gal/Raf
PGal1
PGal1-BRL1
PGal1-brl1F391E
PGal1-brl1F391P
PGal1-brl1C343Y
PGal1-brl1F391E C343Y
PGal1-brl1C365S C371S
PGal1-brl1F391E C365S C371S
PGal1-brl1Y347H
PGal1-brl1F391E Y347H
PGal1-brl1A360D
PGal1-brl1F391E A360D
PGal1-brl1W368Y
PGal1-brl1F391E W368Y
PGal1-brl1N353D
PGal1-brl1F391E N353D
PGal1-brl1T355A
PGal1-brl1F391E T355A
PGal1-brl1P356G
PGal1-brl1F391E P356G
D
dsRED-HDEL
0 h
3 h
E
Along the NE
PGAL1-brl1F391E
NE
F
Released from the NE into the cytoplasm
PGAL1-brl1F391E
NE

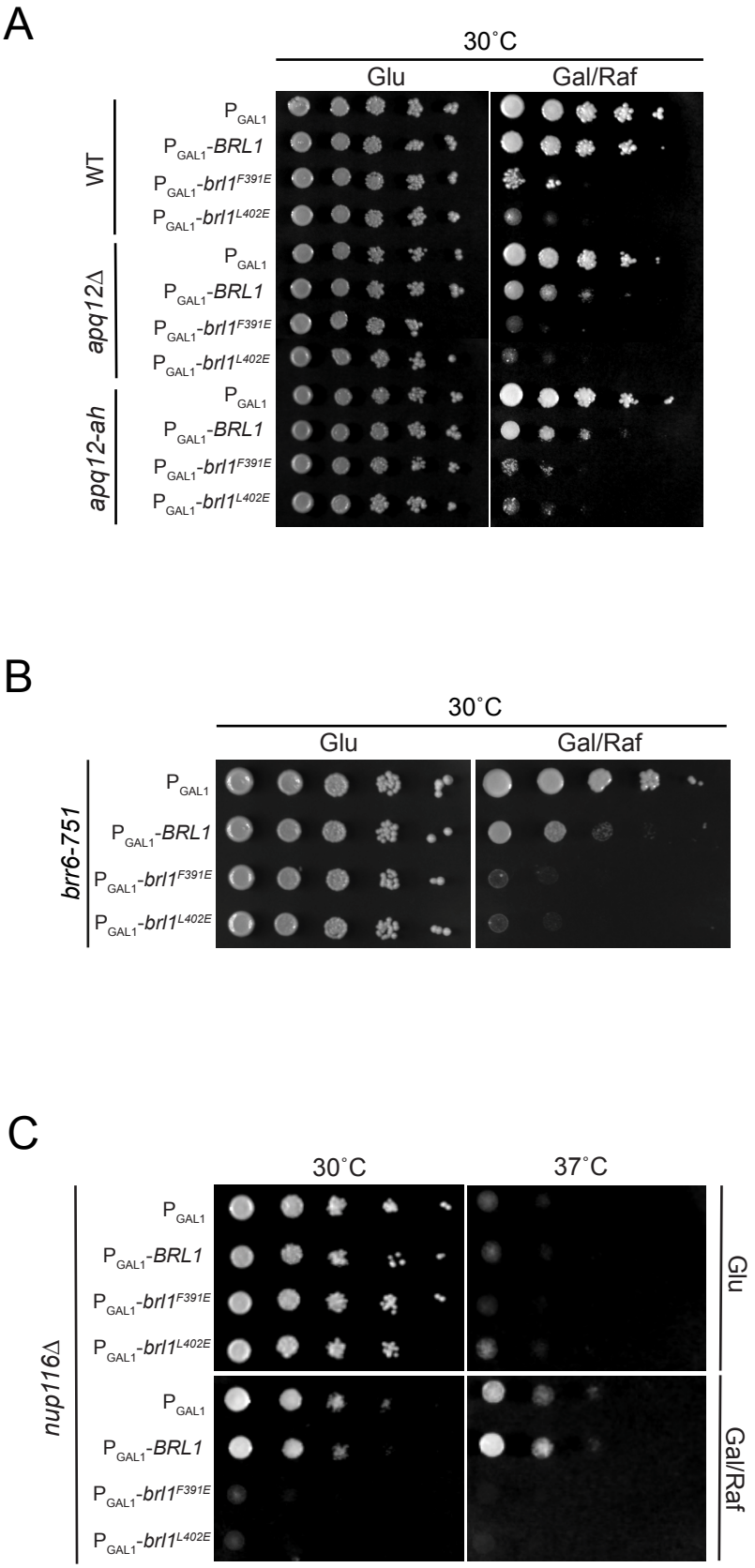
A
30˚C
Glu
Gal/Raf
WT
apq12Δ
apq12-ah
P GAL1
P GAL1-BRL1
P GAL1-brl1F391E
P GAL1-brl1L402E
B
30˚C
Glu
Gal/Raf
brr6-751
C
30˚C
37˚C
nup116Δ
Glu
Gal/Raf

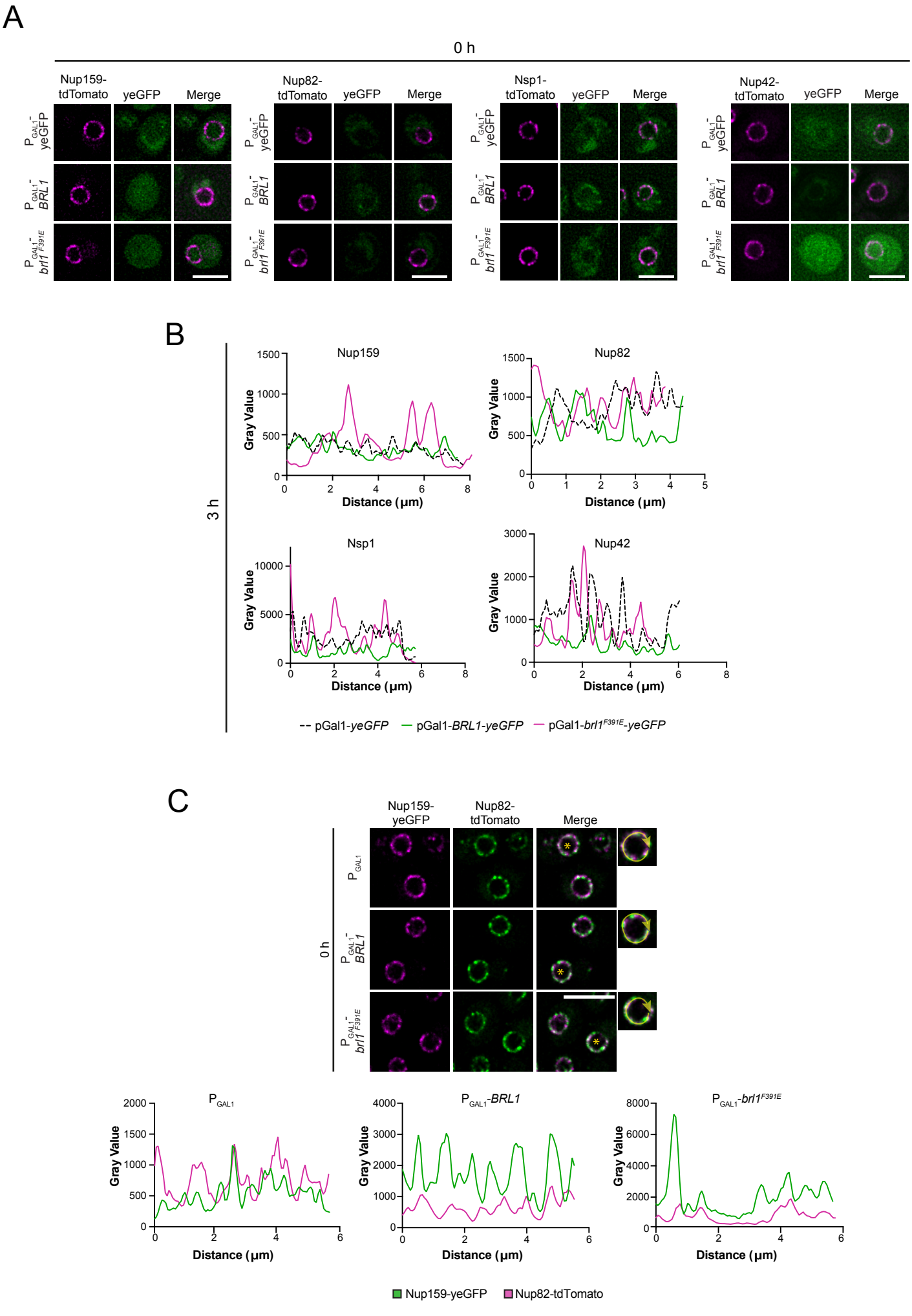
A
0 h
Nup159-tdTomato
yeGFP
Merge
Nup82-tdTomato
Nsp1-tdTomato
Nup42-tdTomato
P GAL1 - yeGFP
P GAL1 - BRL1
P GAL1 - brl1 F391E
B
3 h
Nup159
Nup82
Nsp1
Nup42
Gray Value
Distance (μm)
-- pGal1-yeGFP
pGal1-BRL1-yeGFP
pGal1-brl1F391E-yeGFP
C
Nup159-yeGFP
Nup82-tdTomato
Merge
0 h
P GAL1
P GAL1-BRL1
P GAL1-brl1F391E
Nup159-yeGFP
Nup82-tdTomato

Figure S5

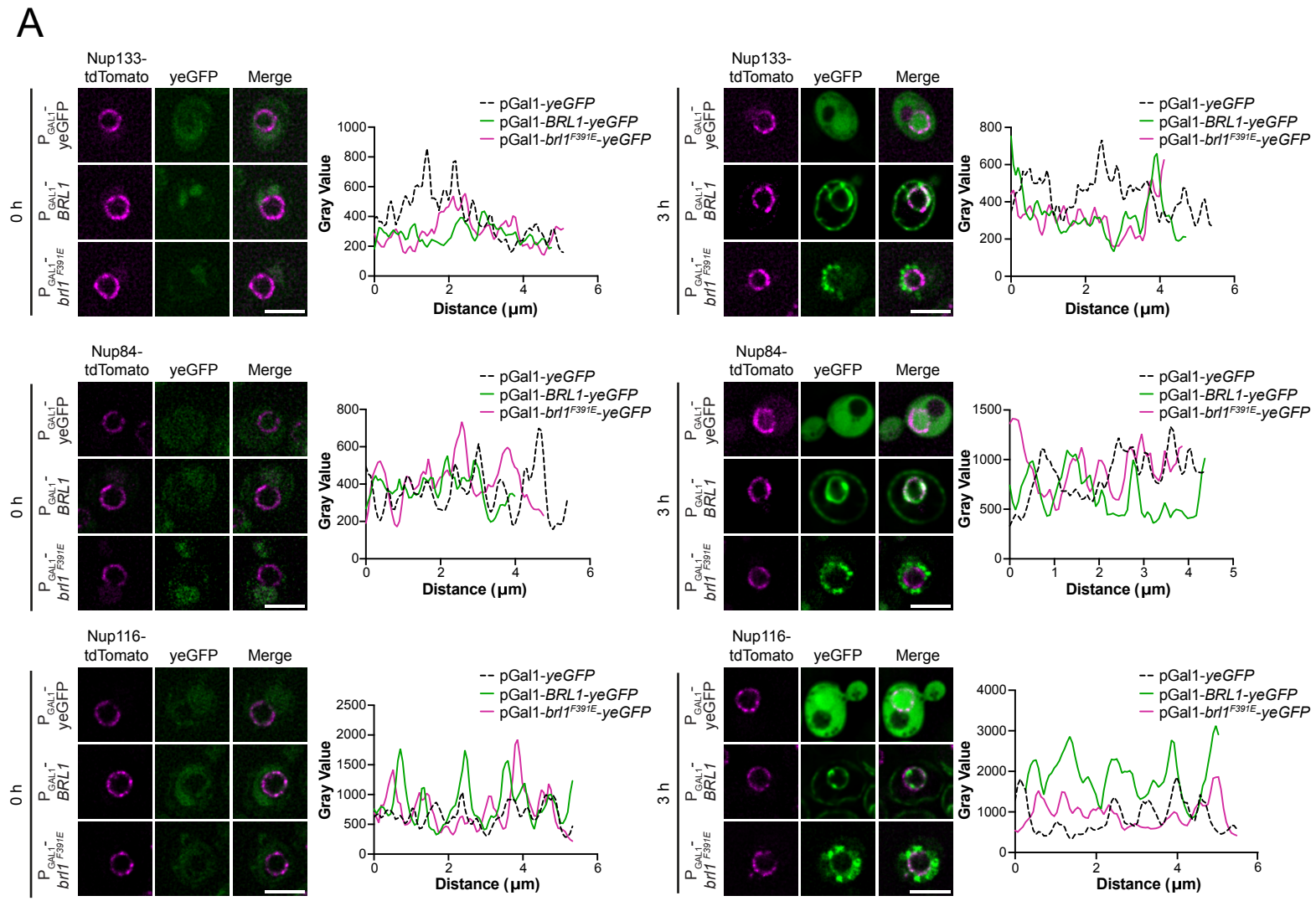
A
Nup133-tdTomato
yeGFP
Merge
0 h
3 h
Nup84-tdTomato
Nup116-tdTomato
Gray Value
Distance (μm)
pGal1-yeGFP
pGal1-BRL1-yeGFP
pGal1-brl1F391E-yeGFP

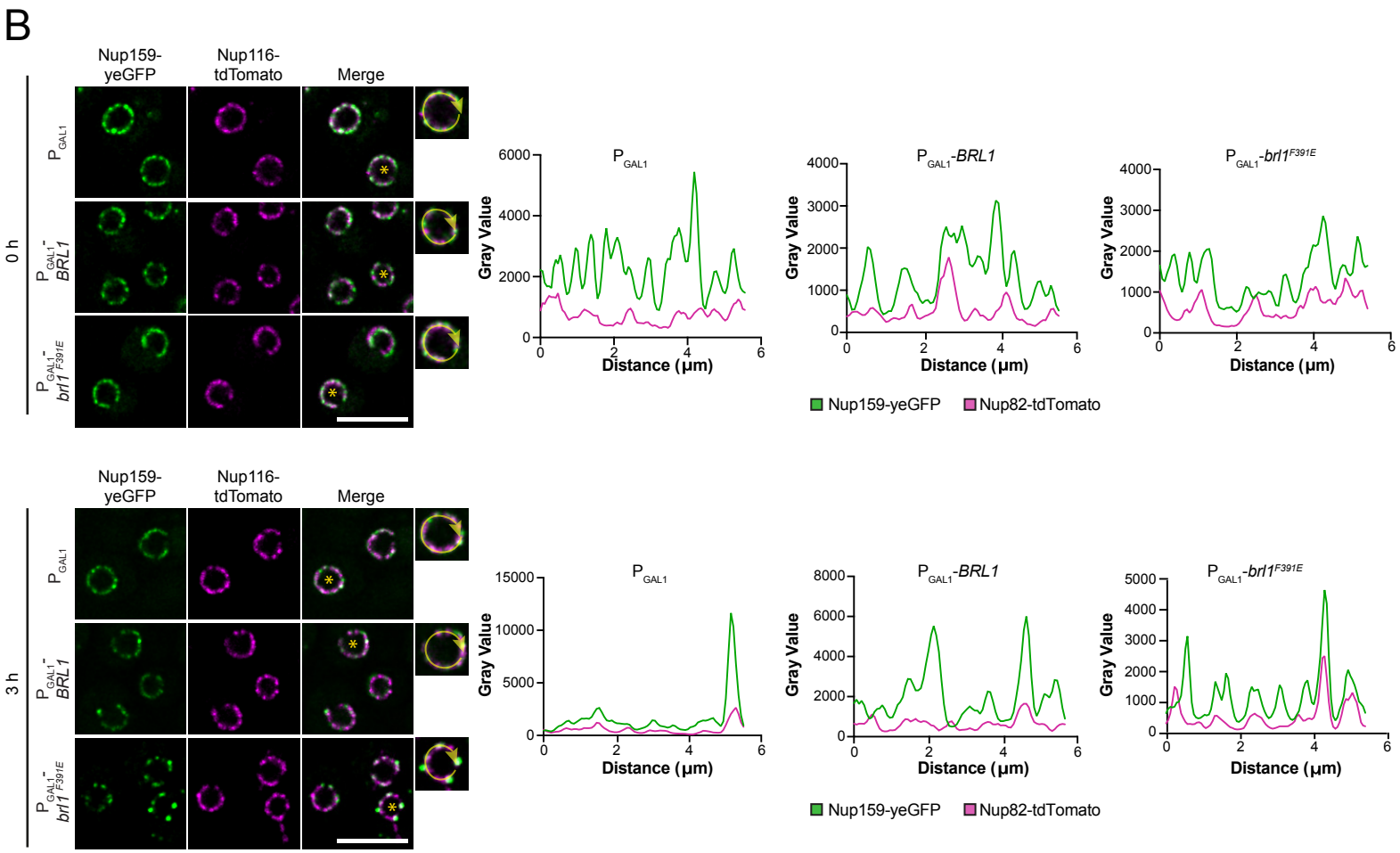
B
Nup159-yeGFP
Nup116-tdTomato
Merge
0 h
3 h
Gray Value
Distance (μm)
Nup159-yeGFP
Nup82-tdTomato

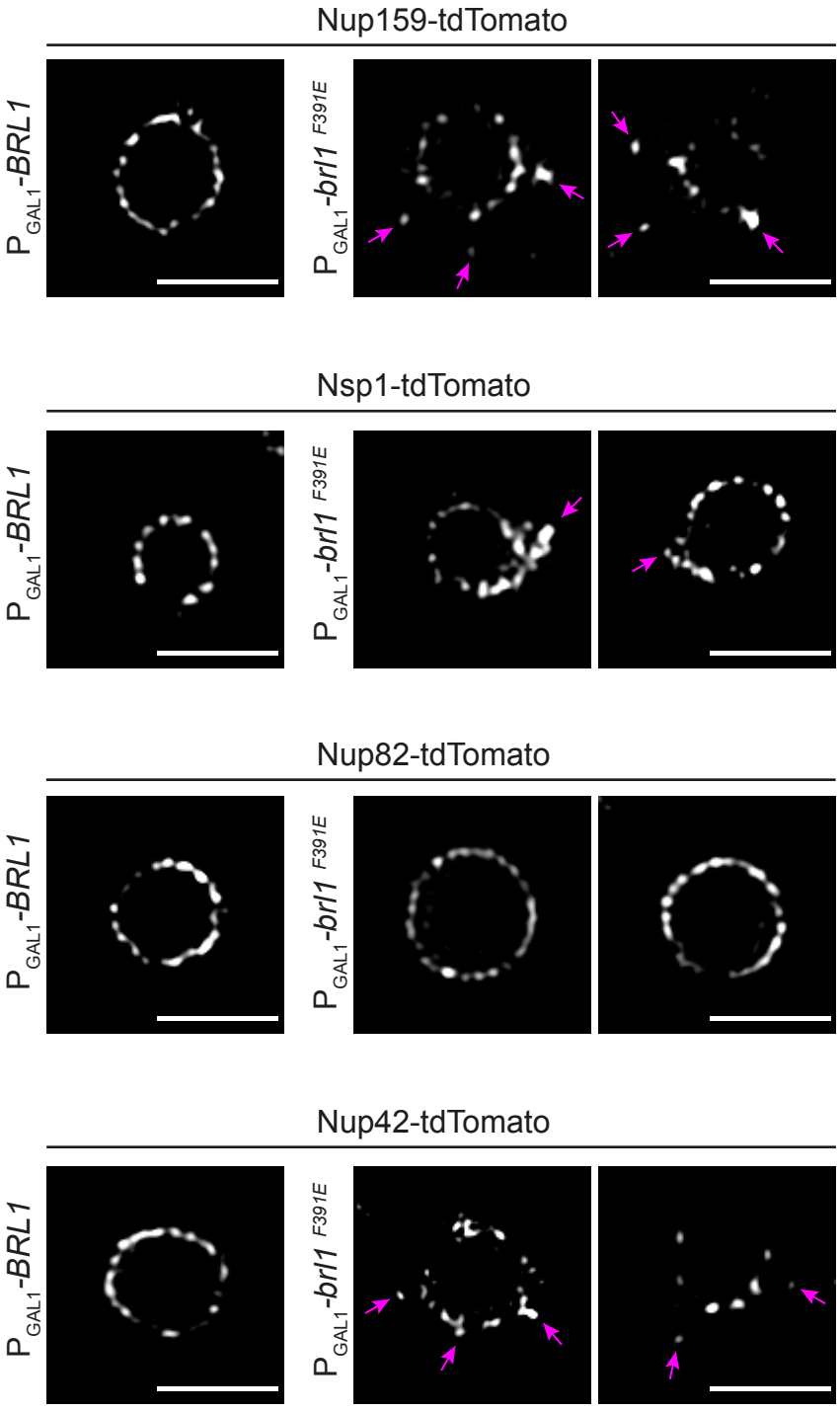
Nup159-tdTomato
Nsp1-tdTomato
Nup82-tdTomato
Nup42-tdTomato
P GAL1 -BRL1
P GAL1 -brl1 F391E

A

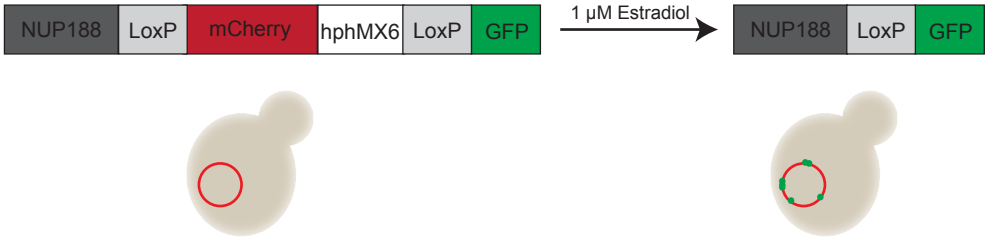
NUP188
LoxP
mCherry
hphMX6
LoxP
GFP
1 μM Estradiol
NUP188
LoxP
GFP

B

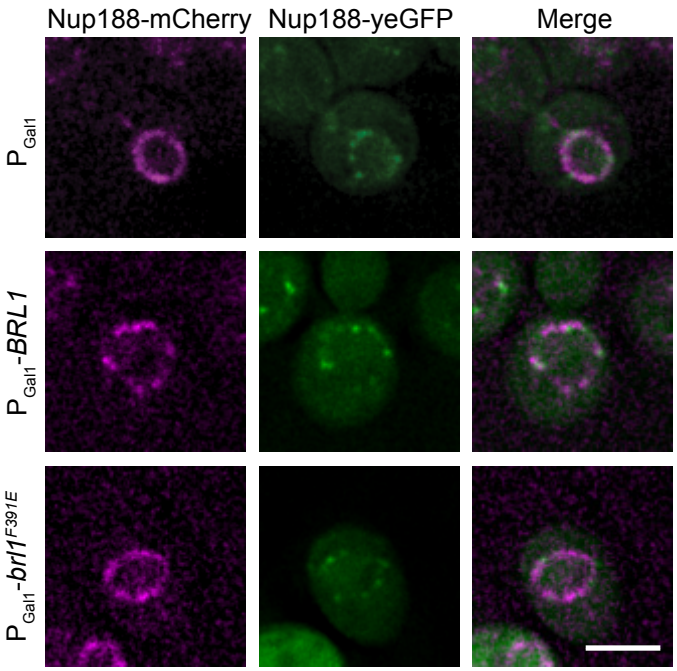
Nup188-mCherry
Nup188-yeGFP
Merge
P Gal1
P Gal1-BRL1
P Gal1-brl1F391E

A

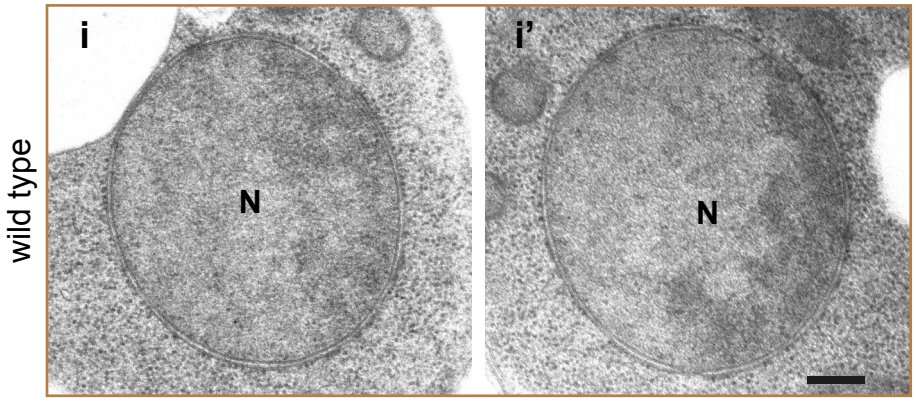
wild type
i
N
i'
N
α-GFP antibody, PAG 15 nm

B

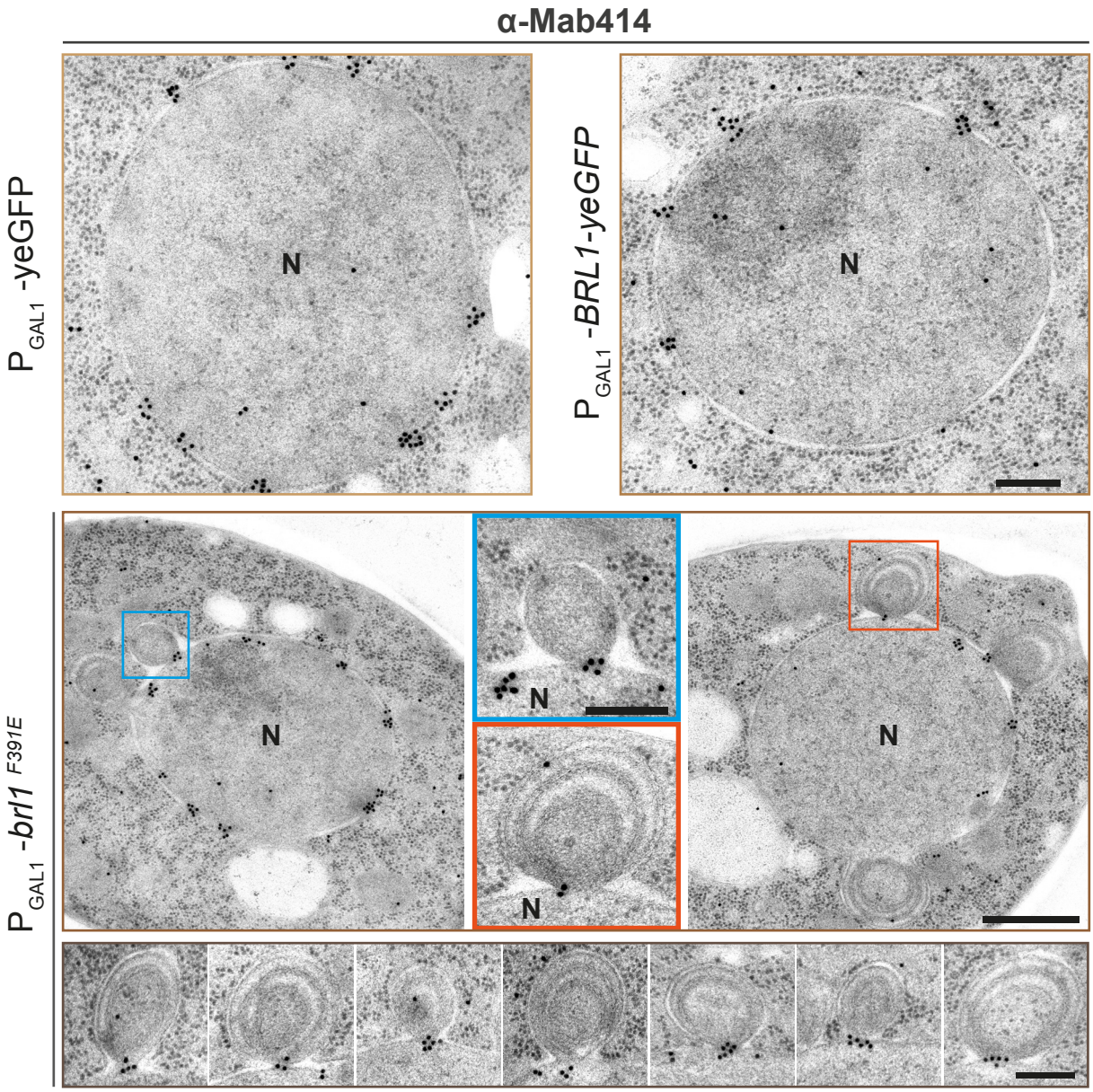
α-Mab414
P GAL1 -yeGFP
N
P GAL1 -BRL1-yeGFP
N
P GAL1 -brl1 F391E
N
N
N
N

Table S1: Yeast strains and plasmids used in this study.

Strain ID	Description	Source/Reference	Figure
	ESM356-1		Fig. 2A, B, 3A, 5A, B, C, S1A, S2A, B, D, E, S7
YZW873	*MATa ura3-52 leu2Δ1 his3Δ200 trp1Δ63 apq12Δ::NatNT2*	Zhang et al., 2021	Fig. S1A
YZW952	*MATa ura3-52 leu2Δ1 his3Δ200 trp1Δ63 apq12-ah-NatNT2*	Zhang et al., 2021	Fig. S1A
AAK0031	*MATa ura3-52 leu2Δ1 his3Δ200 trp1Δ63::YIPlac-dsRED-HDEL-NATMX Rpl25-GFP-klTRP1*	Zhang et al., 2021	Fig. 3B
YZW292	*MATa ura3-52 leu2Δ1 his3Δ200 trp1Δ63::YIPlac-dsRED-HDEL-NatMX*	This study	Fig. 2C, E, S2C
YZW320	MATa ura3-52 leu2Δ1 his3Δ200 trp1Δ63 UBR1::pGal1-HA-UBR1-His3MX6 Nup188-loxP-HA-mCherry-HphMX6-loxP-GFP	Zhang et al., 2018	Fig. S6B
YZW769	MATa ura3-52 leu2Δ1 his3Δ200 trp1Δ63 Δnup116::HphNT1	Zhang et al., 2018	Fig. S1C
AAK0034	*brl1Δ::KAN*, pRS316-*BRL1,* pRS303N-*brl1^{F391E}*	This study	Fig. 1D
AAK0035	*brl1Δ::KAN,* pRS316-*BRL1,* pRS303N-*brl1^{L402E}*	This study	Fig. 1D
AAK0036	*brl1Δ::KAN,* pRS316-*BRL1,* pRS303N	This study	Fig. 1D
AAK0037	*brl1Δ::KAN,* pRS316-*BRL1,* pRS315-*BRL1*	This study	Fig. 1D
AAK0041	*MATa ura3-52 leu2Δ1 his3Δ200 trp1Δ63::YIPlac-GFP-HDEL-NatMX*	This study	Fig. 3B
YZW14	*MATa ura3-52 leu2Δ1 brr6-751*	Dr. I. Hagan	Fig. S1B
AAK0042	*MATa ura3-52 leu2Δ1 his3Δ200 trp1Δ63 NUP82-tdTomato-hph*	This study	Fig. 4B, S3A
YZW815	*MATa ura3-52 leu2Δ1 his3Δ200 trp1Δ63 NSP1-tdTomato-hph*	This study	Fig. 4B, S3A
YJV075	*MATa ura3-52 leu2Δ1 his3Δ200 trp1Δ63 NUP42-tdTomato-hph*	This study	Fig. 4C, S3A
YJV076	*MATa ura3-52 leu2Δ1 his3Δ200 trp1Δ63 NUP159-yeGFP-TRP1 Nup82-tdTomato-hph*	This study	Fig. 4E, S3C
YJV075	*MATa ura3-52 leu2Δ1 his3Δ200 trp1Δ63 NUP159-yeGFP-TRP1 Nup116-tdTomato-hph*	This study	Fig. S4B
AK723	*MATa ura3-52 leu2Δ1 his3Δ200 trp1Δ63 NUP84-mCherry-KanMX6*	This study	Fig. S4A
AK725	*MATa ura3-52 leu2Δ1 his3Δ200 NUP133-mCherry-KanMX6*	This study	Fig. S4A
AK948	*MATa ura3-52 leu2Δ1 his3Δ200 trp1Δ63 NUP159-mCherry-KanMX6*	This study	Fig. 4B, S3A
Plasmid ID	**Description**	**Source/Reference**	
	pFA6a-*KanMX4*	M. Knop	
pCM45	pFA6a-*tdTomato-KanMX6*	M. Knop	
pCM49	pFA6a-*tdTomato-hphMX6*	M. Knop	
pYM25	*yeGFP-hphNT1*	Janke et al., 2004 [48]	
pZW111	p426Gal-*APQ12-6His*	This study	
pZW112	p425Gal-*apq12-ah-6His*	This study	
pAAK0012	pRS303N-*brl1^{F391E}*	This study	
pAAK0013	pRS303N-*brl1^{L402E}*	This study	
pAAK0014	p425Gal-*brl1^{F391E}*	This study	
pAAK0015	p425Gal-*brl1^{L402E}*	This study	
pAAK0016	p426Gal1-*brl1^{F391E}-yeGFP*	This study	
pAAK0019	p426Gal1-*brl1$^{F391E\ C365S\ C371S}$*	This study	

pJV034	p426Gal1-*brl1*^{N353D}	This study	
pJV035	p426Gal1-*brl1*^{T355A}	This study	
pJV036	p426Gal1-*brl1*^{P355G}	This study	
pJV037	p426Gal1-*brl1*$^{F391E\ N353D}$	This study	
pJV038	p426Gal1-*brl1*$^{F391E\ T355A}$	This study	
pJV039	p426Gal1-*brl1*$^{F391E\ P355G}$	This study	
pZW78	p426Gal1-BRL1	This study	
pKW1219	pRS425-NLS-mRFP1	K. Weis	
pAAK0020	p426Gal1-*brl1*^{F391P}	This study	
pAAK0018	p426Gal1-*brl1*$^{C365S\ C371S}$	This study	
pAAK0021	p426Gal1-*brl1*^{C343Y}	This study	
pAAK0022	p426Gal1-*brl1*$^{C343Y\ F391E}$	This study	
pAAK0027	p426Gal1-*brl1*^{A360D}	This study	
pAAK0028	p426Gal1-*brl1*$^{A360D\ F391E}$	This study	
pAAK0025	p426Gal1-*brl1*^{Y347H}	This study	
pAAK0026	p426Gal1-*brl1*$^{Y347H\ F391E}$	This study	
pAAK0029	p426Gal1-*brl1*^{W368Y}	This study	
pAAK0030	p426Gal1-*brl1*$^{W368Y\ F391E}$	This study	
pJV046	pRS315-*brl1*^{F391P}	This study	
pJV047	pRS315-*brl1*^{C343Y}	This study	
pAAK0031	pRS315-*brl1*$^{C365S\ C371S}$	This study	
pJV044	pRS315-*brl1*^{Y347H}	This study	
pJV045	pRS315-*brl1*^{A360D}	This study	
pJV043	pRS315-*brl1*^{W368Y}	This study	
pJV040	pRS315-*brl1*^{N353D}	This study	
pJV041	pRS315-*brl1*^{T355A}	This study	
pJV042	pRS315-*brl1*^{P356G}	This study	